HHS Public Access

Author manuscript

J Physiol. Author manuscript; available in PMC 2020 December 13.

Published in final edited form as:

J Physiol. 2021 May ; 599(9): 2483–2498. doi:10.1113/JP277459.

Phosphorylation in two discrete tau domains regulates a stepwise process leading to postsynaptic dysfunction

Peter J. Teravskis[1,2], **Breeta R. Oxnard**[3], **Eric C. Miller**[4], **Lisa Kemper**[5], **Karen H. Ashe**[5,6,7], **Dezhi Liao**[1]

[1]Department of Neuroscience, University of Minnesota, Minneapolis, MN 55455, USA

[2]School of Medicine, University of Minnesota, Minneapolis, MN 55455, USA

[3]College of Biological Sciences, University of Minnesota, Minneapolis, MN 55455, USA

[4]Graduate Program in Neuroscience, University of Minnesota, Minneapolis, MN 55455, USA

[5]Department of Neurology, University of Minnesota, Minneapolis, MN 55455, USA

[6]N. Bud Grossman Center for Memory Research and Care, Minneapolis, MN 55455, USA

[7]GRECC, Minneapolis VA Medical Center, Minneapolis, MN 55417, USA

Abstract

Tau protein consists of an N-terminal projection domain, a microtubule-binding domain and a C-terminal domain. In neurodegenerative diseases, including Alzheimer's disease and frontotemporal dementia, the hyperphosphorylation of tau changes its shape, binding partners and resulting function. An early consequence of tau phosphorylation by proline-directed kinases is postsynaptic dysfunction associated with the mislocalization of tau to dendritic spines. The specific phosphorylation sites leading to these abnormalities have not been elucidated. Here, using imaging and electrophysiological techniques to study cultured rat hippocampal neurons, we show that postsynaptic dysfunction results from a sequential process involving differential phosphorylation in the N-terminal and C-terminal domains. First, tau mislocalizes to dendritic spines, in a manner that depends upon the phosphorylation of either Ser396 or Ser404 in the C-terminal domain. The blockade of both glycogen synthetase kinase 3β and cyclin-dependent kinase 5 prevents tau mislocalization to dendritic spines. Second, a reduction of functional AMPA receptors depends upon the phosphorylation of at least one of five residues (Ser202, Thr205, Thr212, Thr217 and Thr231) in the proline-rich region of the N-terminal domain. This is the first report of differential phosphorylation in distinct tau domains governing separate, but linked, steps leading to synaptic dysfunction.

Correspondence author D. Liao: Department of Neuroscience, University of Minnesota, Minneapolis, MN 55455, USA. liaox020@umn.edu.

Author contributions

P.J.T., D.L. and K.H.A. designed the experiments and wrote the manuscript. P.J.T., E.M., B.R.O, L.K. and D.L. cloned the constructs and performed electrophysiological and imaging experiments. All authors have read and approved the final version of this manuscript and agree to be accountable for all aspects of the work in ensuring that questions related to the accuracy or integrity of any part of the work are appropriately investigated and resolved. All persons designated as authors qualify for authorship, and all those who qualify for authorship are listed.

Competing interests

None

Introduction

Increasing evidence supports a key role of tau in mediating synaptic and cognitive dysfunction in Alzheimer's disease and other tauopathies (Tracy & Gan, 2018). Tauopathies are neurodegenerative diseases characterized by intraneuronal inclusion bodies composed of hyperphosphorylated species of tau (McKee *et al.* 2009; Ghetti *et al.* 2015; Montenigro *et al.* 2015). These inclusions are frequently associated with dementia in disorders such as Alzheimer's disease (Braak *et al.* 2011), frontotemporal dementia (Ghetti *et al.* 2015) and chronic traumatic encephalopathy (McKee *et al.* 2009; Montenigro *et al.* 2015). The precise sequence of pathophysiological events leading from mild cognitive deficits to overt clinical dementia remains unclear. The early phases of the disease likely involve disturbances of the balanced modulation of synaptic strength at glutamatergic synapses, followed by disruption of synaptic structures, neuritic retraction, and ultimately neurotoxicity leading to cell death and overt clinical dementia (Tracy & Gan, 2018).

In order to identify signalling pathways that contain promising therapeutic targets, numerous functional and molecular studies have focused upon synapses in cellular and mouse models of tauopathies (Santacruz *et al.* 2005; Hoover *et al.* 2010; Ittner *et al.* 2010; Min *et al.* 2010; Lasagna-Reeves *et al.* 2011; Maday *et al.* 2014; Sherman *et al.* 2016; Tracy *et al.* 2016; Zhao *et al.* 2016; Sealey *et al.* 2017; Zhou *et al.* 2017; Mclnnes *et al.* 2018). As tau is enriched in the axons of healthy neurons, it is not surprising that, in some models of disease, tau has been shown to interfere with molecular pathways in axonal transport (Maday *et al.* 2014; Sherman *et al.* 2016) as well as the release of presynaptic vesicles (Sherman *et al.* 2016; Zhou *et al.* 2017; Mclnnes *et al.* 2018). In diseased neurons, tau is found in higher concentrations in the soma and dendrites (Kowall & Kosik, 1987; Avila *et al.* 2004). When it is present in dendrites, tau can mislocalize to postsynaptic structures, namely the dendritic spines. This mislocalization of tau is currently believed to be an important mechanism underlying tau-mediated synaptic and cognitive deficits (Zempel & Mandelkow, 2014; Tracy & Gan, 2018).

The long-lasting synaptic plasticity defects that are associated with neurological disorders commonly feature a dysregulation of glutamatergic AMPA receptors in the postsynaptic membrane of dendritic spines (Hoover *et al.* 2010; Ittner *et al.* 2010; Kam *et al.* 2010; Miller *et al.* 2014; Zhao *et al.* 2016). Recently, reports have linked soluble, post-translationally modified forms of tau, either directly or indirectly, to defects in AMPA receptor trafficking (Hoover *et al.* 2010; Sydow *et al.* 2011). Some of the post-translational modifications that have been described are phosphorylation by proline-directed kinases (Hoover *et al.* 2010), cleavage by caspase-2 (Zhao *et al.* 2016), and acetylation by major tau acetyltransferases p300 and CREB-binding protein (CBP) (Min *et al.* 2010; Tracy *et al.* 2016). Tau phosphorylation has been associated with AMPA receptor reduction in the postsynaptic membrane of dendritic spines, as well as tau mislocalization to dendritic spines (Hoover *et al.* 2010; Ittner *et al.* 2010; Miller *et al.* 2014; Zhao *et al.* 2016). Still unknown is whether tau mislocalization to dendritic spines alone is sufficient to cause AMPA receptor loss. Furthermore, it is unclear whether this mislocalization is initiated by specific tau

phosphorylation sites or by a non-specific change in electrical charge (due to the addition of negatively charged phosphates) throughout the entire tau molecule.

In this paper, we report the effects of multi-regional phosphorylation of tau on synaptic dysfunction using imaging and electrophysiological methods. Our results indicate that tau mislocalization to dendritic spines depends on phosphorylation of residues in the C-terminal domain, whereas a reduction of AMPA receptors in the postsynaptic membrane of dendritic spines requires the phosphorylation of residues in the proline-rich region of tau in the N-terminal domain. Our novel results demonstrate for the first time that differential phosphorylation in distinct tau domains governs separate but linked processes that lead to tau mislocalization and subsequent postsynaptic dysfunction.

Methods

Ethical approval

All work was conducted in accordance with the American Association for the Accreditation of Laboratory Animal Care and Institutional Animal Care and Use Committee (IACUC) at the University of Minnesota (protocol no.1211A23505). Animals were euthanized by decapitation using inhaled carbon dioxide anaesthesia. We performed all procedures of euthanasia and anaesthesia strictly according to the guidelines of the IACUC at the University of Minnesota. In carbon dioxide anaesthesia, rats were put in a standard rat cage (L48 × W25 × H19 cm), which would be subsequently connected with a tube and a flow meter to a gas tank of carbon dioxide. The flow rate was adjusted so that it would not displace any more than 30% of the cage volume per minute. The gas flow would continue until the animals no longer displayed the pedal reflex (firm toe pinch).

Materials

All common chemical reagents and cell culture supplies were purchased from Sigma-Aldrich (St Louis, MO, USA), Promega (Madison, WI, USA) and Thermo-Fisher Scientific (Waltham, MA, USA)/Invitrogen/Life Technologies unless otherwise indicated.

Plasmids

All human tau and DsRed constructs were expressed in the pRK5 vector and driven by the cytomegalovirus promotor (Clontech Inc., Takara Bio Inc, Mountain View, CA, USA). All human tau was N-terminally fused to enhanced green fluorescent protein (eGFP). The wild-type, native human tau construct encoded human four-repeat tau lacking the transcriptional variant N-terminal sequences (0N4R) and contained exons 1, 4, 5, 7, 9–13, 14 and intron 13 (RRID:Addgene_46904). P301L mutant as well as alanine and glutamate tau variant constructs were created using step-wise site-directed mutagenesis (QuikChange SDM Kit, Agilent Technologies, Santa Clara, CA, USA). PCR primers for mutagenesis were 15–22 nucleotides long, centred on mutated nucleotide(s) (Integrated DNA Technologies, Coralville, IA, USA). All nucleotide mutations as well as plasmid construct integrity were confirmed with Sanger Sequencing (UMN Genomics Centre, Minneapolis, MN, USA). Tau sequence numbering was based on the longest functional human isoform: 441-tau (2N4R tau; NCBI reference sequence: NP_005901.2).

Primary hippocampal neuron cultures

Briefly, a 22 mm diameter glass coverslip (0.09 mm thickness) was silicone-sealant-fastened to the bottom of a 35 mm culture dish with a bored hole of 20 mm in diameter and sterilized as we previously described (Lin *et al.* 2004). Coverslips were coated with poly-D-lysine. Hippocampi were dissected from CO_2-anaesthetized neonatal Sprague–Dawley timed-pregnancy rats (Envigo, Indianapolis, IN, USA) at 0–24 h of life. Rats were fed a diet of regular chow, *ad libitum*. Hippocampi were enzymatically digested in Earle's balance salt solution (EBSS) supplemented with 1% glucose and cysteine-activated papain. Digestion was blocked with dilute DNase, and cells were rinsed in fresh EBSS and plated in plating medium (minimal essential medium with Earle's salts, 10% fetal bovine serum, 5% horse serum, 2 mM glutamine, 10 mM sodium pyruvate, 0.6% glucose, 100 U ml^{-1} penicillin and 100 mg ml^{-1} streptomycin) at 1.0×10^6 cells/dish. After 18 h, cell adherence was established. Cells were then grown in neurobasal medium (NbActiv1; BrainBits LLC, Springfield, IL, USA) and incubated at 37°C in a 5% CO_2 biological incubator.

Low efficiency calcium-phosphate transfection

At 5–7 days *in vitro* (DIV) cells were transfected. DNA plasmid transfection was performed using standard calcium phosphate precipitation and incubation as we previously described (Liao *et al.* 2005). Briefly, neurons were transfected with human tau constructs and DsRed (2:1 by plasmid DNA mass) for live imaging, and with human tau alone for electrophysiology and immunocytochemistry. Precipitated DNA was applied to cells in a solution of glial conditioned medium (neurobasal medium previously conditioned for 14 days on a glial monolayer and reserved) containing 100 μM DL-2-Amino-5-phosphonopentanoic acid (APV) to prevent calcium-induced excitotoxicity. After 3–4 h transfection time, cells were rinsed in glial conditioned medium and grown in neurobasal medium as described above until mature (21–28 DIV).

Electrophysiolology

Miniature excitatory postsynaptic currents (mEPSCs) were recorded from cultured dissociated rat hippocampal neurons at 21–25 DIV with a glass pipette (resistance ~5 MΩ) at holding potentials of −65 mV on an Axopatch 200B amplifier (Molecular Devices, San Jose, CA, USA; output gain = 1; filtered at 1 kHz) as we previously described (Hoover *et al.* 2010). Input and series resistances were assessed and found to have no significant difference before and after recording time (5–20 min). Recording sweeps lasted 200 ms and were sampled for every 1 s (pClamp, v10, RRID:SCR_011323; Molecular Devices). Neurons were bathed in bubble-oxygenated artificial cerebral spinal fluid (ACSF) at 23°C with 100 μM APV (NMDA receptor antagonist), 1 μM tetrodotoxin (TTX; sodium channel blocker) and 100 μM picrotoxin ($GABA_A$ receptor antagonist). Passive oxygen perfusion was established with medical-grade 95% O_2–5% CO_2. ACSF contained (in mM): 119 NaCl, 2.5 KCl, 5.0 $CaCl_2$, 2.5 $MgCl_2$, 26.2 $NaHCO_3$, 1 NaH_2PO_4 and 11 D-glucose. The internal solution of the glass pipettes contained (in mM): 100 caesium gluconate, 0.2 EGTA, 0.5 $MgCl_2$, 2 ATP, 0.3 GTP and 40 Hepes. The pH of internal solution was normalized to 7.2 with caesium hydroxide and diluted to a trace osmotic deficit in comparison to ACSF (~300 mOsm). All analysis of recordings was performed manually (Mini Analysis Program,

v6.0.7, RRID:SCR_002184; Synaptosoft Inc., Fort Lee, NJ, USA). Minimum analysis parameters were set at greater than 1 min stable recording time and event amplitude greater than 2 pA. A mEPSC event was identified by distinct fast-rising depolarization and slow-decaying repolarization. Combined individual events were used to form relative cumulative frequency curves, whereas the means of all events from individual recordings were treated as single samples for further statistical analysis. Example traces were exported from Mini Analysis and live-traced, simplified, and united in vector editing software (Adobe Illustrator CS5, v15, RRID:SCR_010279).

Image analysis of live neuronal cultures

Transfected cells were continually bathed in neurobasal media and were passively perfused with medical-grade 95% O_2–5% CO_2. Micrographs were taken on a Nikon epifluorescence inverted microscope with ×60 oil lens with a computerized focus motor at DIV 21–23. All digital images were processed using microscopic imaging software (MetaMorph Microscopy Automation and Image Analysis Software, v7.1, RRID:SCR_002368, MetaMorph Inc., Nashville, TN, USA). Images were taken as 15 plane stacks at 0.5 μm increments, processed by deconvolution to the nearest planes, and averaged against other stacked images. A dendritic spine was defined as having an expanded head diameter, greater than 50% larger in diameter than the neck. The number of spines per neuron was counted and normalized to a 100 μm length of dendritic shaft.

Pharmacology

Roscovitine and CHIR99021 were purchased from Sigma-Aldrich and were diluted in DMSO to four 1000× concentration aliquots for ultimate concentrations in neurobasal medium of 0.05, 0.5, 5 and 10 μM. Primary cultured rat hippocampal neurons transfected with DsRed and eGFP-P301L-tau were treated with one of four 1000× aliquots or DMSO vehicle on DIV 20–22. Treated cells were incubated for 24 h prior to imaging on DIV 21–23. Cell death was visually assessed under differential interference contrast (DIC) for decreased cell density, lost soma adhesion, and gross qualitative neurite retraction. If evidence of cell death was observed under DIC, cells were fixed in 4% sucrose and 4% paraformaldehyde in phosphate-buffered saline (PBS) and stained with 300 nM 4′,6-diamidino-2-phenylindole (DAPI) in PBS. DAPI-stained cells were analysed under fluorescence microscopy for nuclear pyknosis and karyorrhexis; DsRed expressing cells were analysed for spine loss. If no cell death was evident under DIC, live fluorescence images were acquired and analysed as above.

Immunocytochemistry

Cultured neurons were fixed and permeabilized with 4% paraformaldehyde + 4% sucrose (23°C, 30 min), 100% methanol (−20°C, 20 min) and 0.2% Triton X-100 (23°C, 20 min) applied successively as previously described (Lin *et al.* 2004). Cells were blocked with 10% normal goat serum (NGS) at room temperature for 20 min (Jackson ImmunoResearch Laboratories, West Grove, PA, USA, cat. no. 005-000-121). Neurons were co-incubated with a primary mouse monoclonal AT8 anti-phospho-tau antibody (Thermo Fisher Scientific, cat. no. MN1020, RRID: AB_223648; targeting phospho-S202 and phospho-T205 residues; diluted at 1:200 in 10% NGS) (Goedert *et al.* 1995), and a primary rabbit polyclonal anti-

GFP antibody (to compensate for decreased eGFP signal due to fixation; Thermo Fisher Scientific, cat. no. A-11122, RRID:AB_221569; diluted at 1:200 in 10% NGS) at room temperature overnight. The neurons were washed with PBS three times and subsequently incubated with two secondary antibodies from Jackson Immuno-Research Laboratories (goat rhodamine anti-mouse, cat. no. 111-025-003, RRID:AB_2337926; and goat fluorescein isothiocyanate tagged anti-rabbit, cat. no. 111-095-003, RRID:AB_2337972) at a dilution of 1:200 in 10% NGS for 1 h. Fluorescence intensity was derived from peak pixel intensity taken at the centre of a soma or the middle of a dendrite branch and normalized by dividing by pixel intensity of adjacent background fluorescence using Metamorph software (MetaMorph Inc.).

Statistics and figure design

All statistics were performed in biological statistical analysis software (Prism, v6, RRID:SCR_002798, GraphPad Software Inc., La Jolla, CA, USA). We utilized one- and two-way ANOVA for univariate and multivariate analysis, respectively. If ANOVA revealed significant variance between all groups, *post hoc* analysis was performed using Bonferroni analysis adjusted for multiple groups. Univariate cumulative frequency distributions were compared using the unmodified Kolmogorov–Smirnov goodness-of-fit (GOF) test. Single comparisons were analysed using Student's *t* test. For all, statistical significance was set for $\alpha = 0.05$. Data representations are described in respective figure legends. Figures were designed and created using Adobe Photo-shop CS5 (v12, RRID:SCR_014199) for raster images and Affinity Designer (v1.6.1, RRID:SCR_016952, Serif (Europe) Ltd., Nottingham, UK) for vector images.

Results

Phosphorylation is one of the most common post-translational modifications of tau in tauopathies. It has been associated with both a reduction of AMPA receptors in the postsynaptic membrane of dendritic spines and the mislocalization of tau to dendritic spines (Hoover *et al.* 2010; Ittner *et al.* 2010; Miller *et al.* 2014). Here, we systematically mutated tau to further clarify the relationship between tau phosphorylation and mislocalization. We formulated three domains (designated A-, B- and C-domains) in a balanced, semi-random fashion, each containing clusters of four or five SerPro/ThrPro (SP/TP) residues phosphorylated by proline-directed kinases (Fig. 1*A*; see also the rationale for the initial domain map and its evolution in Fig. 8). Thr111, Thr153, Thr175, Thr181 and Ser199 constitute the A-residues in the A-domain; Ser202, Thr205, Thr212, Thr217 and Thr231 constitute the B-residues in the B-domain; and Ser235, Ser396, Ser404 and Ser422 constitute the C-residues in the C-domain. To determine the differential effects of phosphorylation within each domain, we mutated SP/TP residues in each domain to alanine (Ala) to block phosphorylation and to glutamate (Glu) to mimic phosphorylation, and compared the effects of the variant and native tau proteins. In this study, Pro301-to-Leu (P301L) 'mutant' and 'wild-type' refer to 0N4R tau with and without the P301L mutation, respectively; 'variant' and 'native' refer to tau with and without SP/TP substitutions, respectively. The P301L mutation is associated with frontotemporal dementia with parkinsonism linked to chromosome 17 (Hutton *et al.* 1998).

To identify the phosphorylated residues that regulate the mislocalization of tau, we first tested the effects of blocking phosphorylation in each of the three domains on the subcellular distribution of tau. At 7–10 DIV, we co-expressed DsRed (to visualize cellular morphology) and P301L mutant or wild-type eGFP–tau constructs with alanine substitutions in the A-domain (A-Ala), B-domain (B-Ala) or C-domain (C-Ala) in cultured rat hippocampal neurons. At 21 DIV, we photographed the dendrites of live neurons and determined the percentage of spines containing eGFP–tau. Consistent with prior studies (Hoover *et al.* 2010), we found that eGFP–tau was distributed throughout the dendritic shaft in all conditions, and we found significantly more eGFP-containing spines in neurons expressing P301L mutant eGFP–tau (Fig. 1*B* and *C*). Neurons expressing the A-Ala and B-Ala variants of P301L mutant eGFP–tau showed slight reductions in the percentage of eGFP–tau-containing spines (Fig. 1*B* and *C*), but these changes were not significant when the data were normalized to their respective wild-type tau control groups (Fig. 1*D*). Interestingly, in neurons expressing the C-Ala variant of P301L mutant eGFP–tau, the percentage of eGFP-containing spines dropped dramatically, to the level observed in neurons expressing wild-type eGFP–tau (Fig. 1*B*–*D*). Thus, blocking phosphorylation of SP/TP residues in the C-domain, but not in the A- and B-domains, prevented P301L-induced mislocalization to dendritic spines. We found no change in spine density among the various tau species (Fig. 1*E*), indicating no overt synaptotoxicity associated with mislocalization over the period observed.

We obtained additional support for the conclusion that tau mislocalization depends on C-domain phosphorylation by evaluating the effects of differential phosphorylation in each domain using phosphomimetic variants. Because we found that pseudophosphorylation of the A-residues is neither necessary nor sufficient to mediate tau-induced deficits (Figs 3 and 9), we focused on characterizing the effects of pseudophosphorylation of the B-residues and C-residues. As above, we co-expressed DsRed and P301L mutant or wild-type eGFP–tau constructs with glutamate substitutions in the B-domain (B-Glu) or C-domain (C-Glu) in cultured rat hippocampal neurons and photographed their dendrites to determine the percentage of spines containing eGFP–tau (Fig. 2*A* and *B*). Confirming previous results (Hoover *et al.* 2010), in neurons expressing tau variants that contain the P301L mutation, a high percentage of DsRed labelled spines contained eGFP–tau regardless of the expression of phosphomimetic mutations in B-and C-domains. In the absence of the P301L mutation, neurons expressing native wild-type eGFP–tau showed a low percentage of eGFP-containing spines. Interestingly, expressing the C-Glu variant of wild-type eGFP–tau led to dramatically increased percentages of eGFP-containing spines that were comparable to expressing P301L mutant eGFP–tau (Fig. 2*B*). In contrast, expressing the B-Glu variant of wild-type eGFP–tau did not lead to an increase in eGFP-containing spines. Based upon results in Figs 1 and 2, we concluded that the phosphorylation of one or more C-residues, but not B-residues, induces tau to mislocalize to dendritic spines.

To evaluate the role of phosphorylation in tau-related postsynaptic dysfunction, we tested the effect of separately blocking phosphorylation in each domain on AMPA receptor function. We expressed A-Ala, B-Ala and C-Ala variants of P301L mutant and wild-type eGFP–tau in cultured rat hippocampal neurons and performed whole-cell, patch-clamp electrophysiology to record glutamatergic mEPSCs. In neurons expressing P301L mutant eGFP–tau we found

mEPSCs with smaller amplitudes (Fig. 3*A*, *B* and *D*) and normal frequencies (Fig. 3*C*). Preserved mEPSC frequencies, indicating normal presynaptic function, likely result from the very low transfection efficiency (1–5%) in our experimental system. Low transfection efficiency makes it unlikely that a patched cell would be predominantly innervated by pre-synaptic terminals from a neuron expressing exogenous eGFP–tau. Alanine substitutions in the A-, B- and C-domains produced different effects on postsynaptic dysfunction caused by the P301L mutation. The mEPSCs in neurons expressing the A-Ala variant of P301L mutant eGFP–tau remained abnormally small (Fig. 3*A*, *B* and *E*), indicating that postsynaptic function was not affected by phosphorylation in the A-domain. However, both B-Ala and C-Ala substitutions restored the amplitudes of mEPSCs (Fig. 3*A*, *B*, *F* and *G*). Given that the B-Ala variant of P301L mutant eGFP–tau is abnormally elevated in dendritic spines (Fig. 1*C*), the normal mEPSCs in these neurons is surprising; these data suggest that tau mislocalization alone is not sufficient to induce post-synaptic dysfunction. Therefore, we hypothesize that postsynaptic dysfunction is contingent on mislocalization, which depends on C-domain phosphorylation, in addition to phosphorylation in the B-domain.

To further test the hypothesis that phosphorylation within the B- and C-domains collaborates to disrupt postsynaptic function, we examined the effects of phosphomimetic B-Glu, C-Glu and B+C-Glu on tau-induced glutamatergic postsynaptic function. We accomplished this by measuring mEPSCs in cultured rat hippocampal neurons expressing P301L mutant or wild-type eGFP–tau. As expected, neurons expressing P301L mutant eGFP–tau showed reductions in mEPSC amplitudes, irrespective of phosphomimetic mutations (Fig. 4*A*, *B* and *D*–*G*). However, in neurons expressing wild-type eGFP–tau, neither B-Glu nor C-Glu alone altered mEPSCs (blue and pink lines and symbols, Fig. 4*A*, *B*, *E* and *F*). Interestingly, mEPSC amplitudes were greatly reduced in neurons expressing the B+C-Glu variant of wild-type eGFP–tau (green lines and symbols, Fig. 4*A*, *B* and *G*), indicating that postsynaptic dysfunction depends on phosphorylation in both the B- and the C-domains. Taken together with the results of the phospho-blocking experiments (Figs 1 and 3), we conclude that post-synaptic dysfunction occurs through a coordinated series of events. Specifically, this dysfunction entails C-domain phosphorylation-induced tau mislocalization to spines, and subsequent weakening of AMPA receptor-mediated postsynaptic responses secondary to phosphorylation in the B-domain.

Hyperphosphorylated tau proteins have been reported to be enriched in the somatic and dendritic compartments of neurons from rTg(tauP301L)4510 mice brain tissue (Ramsden *et al.* 2005). However, still unknown is whether the P301L mutation leads to tau hyperphosphorylation also in primary neuronal cultures, and whether the phosphorylation of C-domain residues leads to secondary phosphorylation of B-domain residues. To address that question, we used the AT8 antibody to detect the presence of tau proteins phosphorylated at S202 and T205 in the B-domain. We stained neurons expressing wild-type, P301L or C-Glu eGFP–tau (Fig. 5), and found strong AT8 staining in the somas, dendrites and dendritic spines of neurons expressing P301L eGFP–tau (Fig. 5*A* and *C*). Neurons expressing wild-type tau or C-Glu eGFP–tau had weakly staining somas (Fig. 5*A*), and almost no staining in dendrites (Fig. 5*C*). Quantitatively, the fluorescence intensity of AT8 staining in somas and dendrites in P301L eGFP–tau-expressing neurons was significantly higher than in neurons expressing wild-type or C-Glu eGFP–tau (Fig. 5*B* and

D). These results confirm that the P301L mutation induces hyperphosphorylation of B-domain residues in primary neuronal cultures. By contrast, the weak AT8 staining in neurons expressing C-Glu eGFP–tau does not differ significantly from that in neurons expressing wild-type eGFP–tau (Fig. 5*B* and *D*). Thus, pseudophosphorylation of C-domain residues does not induce secondary phosphorylation of at least two B-domain residues.

Based on previously reported 2D-phosphopeptide mapping of purified cell lysates (Illenberger *et al.* 1998; Kimura *et al.* 2014; Tenreiro *et al.* 2014), among the residues in the C-domain, S235 and S404 are phosphorylated by cyclin-dependent kinase 5 (CDK5) whereas S396 (dominant site) and S404 (minor site) are phosphorylated by glycogen synthetase kinase 3β (GSK3β) (illustrated in Fig. 6*A*). To determine the roles of the two tau kinases in tau mislocalization to dendritic spines, we first treated neurons expressing P301L mutant eGFP–tau with CHIR99021, a GSK3β inhibitor, and roscovitine, a CDK5 inhibitor at the concentrations of 0.05, 0.5 and 5 μM (Fig. 6*B–D*). We found that the treatment of either drug alone reduce tau mislocalization to some degree (Fig. 6*B–D*). However, at concentrations up to 5 μM, neither drug alone lowered the percentage of eGFP-containing spines to control levels (Fig. 6*B–D*). Concentrations of CHIR99021 above 5 μM led to overt cell death (data not shown). In contrast, treating neurons expressing P301L mutant eGFP–tau with a combined 500 nM CHIR99021 and 500 nM roscovitine reduced the percentage of eGFP-containing spines to that of wild-type eGFP–tau (Fig. 6*D–E*). These results indicate that the inhibition of both kinases is necessary to suppress mislocalization, and GSK3β and CDK5 act as redundant activators of a signalling cascade that ultimately leads to synaptic deficits. The treatment with either or both drugs did not significantly change the density of dendritic spines (Fig. 6*F*).

Based on the above pharmacological studies, we hypothesized that S235, S396 and S404 are involved in tau mislocalization to dendritic spines. To refine the identification of C-residues responsible for mislocalization, we mutated the above three residues as well as S422, which is phosphorylated by mitogen-activated protein kinase kinase 4 (MKK4) (Grueninger *et al.* 2011), to alanine residues in multiple combinations (Fig. 7*A*). P301L mutant tau-induced mislocalization was blocked to the same extent with S396A:S404A as with S235A:S396A:S404A:S422A, suggesting that simultaneous blockade of the phosphorylation of only two residues, S396 and S404, is required to ameliorate the tau-induced abnormalities. S235A:S396A:S404A also blocked tau mislocalization, excluding a role for S422 phosphorylation in mislocalization (Fig. 7*A*). As the S235 residue is located within the proline-rich region of tau, we sought to exclude its involvement in inducing synaptic deficits (Figs 1*A* and 7*B–D*). We expressed a wild-type eGFP–tau variant pseudophosphorylated at all five B-domain residues along with residues S396, S404 and S422 in the C-domain, but with the phosphorylation-blocking S235A mutation in the proline-rich region. Electrophysiological analysis of neurons expressing this variant revealed significant reductions in mEPSC event amplitude, but no functional differences compared to the B+C-Glu eGFP–tau variant (Fig. 7*B–D*). Taken altogether, these results indicate that phosphorylation at either S396 or S404 is sufficient to induce tau mislocalization to dendritic spines and that phosphorylation of S235 is not necessary to induce postsynaptic signalling deficits.

Discussion

Our current study shows that postsynaptic dysfunction is the result of a coordinated progression of differential phosphorylation along a common pathway, as depicted in our conceptual model (Fig. 7*E*). Our reduction of tau hyperphosphorylation into three functional phosphorylation domains permitted us to deduce that tau mislocalization to spines and decreased AMPA receptor signalling take place along one common pathway. This process further enabled us to identify the individual residues in the C-terminal tail and the residues in the proline-rich domain that govern tau-induced postsynaptic dysfunction.

In cultured neurons, preventing the phosphorylation of both S396 and S404 reduced tau mislocalization to dendritic spines. In addition, the phosphorylation of either S396 or S404 in the C-terminal tail is both necessary and sufficient to induce tau mislocalization to dendritic spines (Fig. 7*E*). Either blocking tau mislocalization or blocking the phosphorylation of B-residues (S202, T205, T212, T217, T231) prevented the reduction of mEPSC amplitudes.

An interesting question concerning the B-domain residues is: are they phosphorylated before or after they enter the dendritic spines? In P301L eGFP–tau-expressing neurons, we found abundant AT8 staining, which detects the phosphorylation of S202 and S205 in the B-domain, in somas, dendrites and dendritic spines (Fig. 5). Therefore, it is likely that the B-domain residues are phosphorylated prior to mislocalizing to dendritic spines (Fig. 7*E*).

The exact upstream factors that cause cellular stress and consequent pathological activation of kinases are unknown. The unfolded protein response that is activated by endoplasmic reticulum (ER) stress (Lai *et al.* 2007; Su *et al.* 2016) was shown to increase phosphorylation of the S202 and S205 residues in the B-domain (Kim *et al.* 2017). It was also reported that ER stress activates GSK3β (Liu *et al.* 2016). The dysregulation of CDK5, which phosphorylates the C-residue S404, and GSK3β, which predominantly phosphorylates the C-residue S396, is implicated in the pathogenesis of Alzheimer's disease (Patrick *et al.* 1999; Bhat *et al.* 2004; Shukla *et al.* 2012).

The signalling cascade downstream from tau likely involves alterations in its binding partners resulting from phosphorylation in the B- and C-domains. One potential binding partner involved is calcineurin. This phosphatase mediates AMPA receptor endocytosis occurring in long-term depression, a form of long-lasting synaptic plasticity underlying memory formation (Dell'Acqua *et al.* 2006; He *et al.* 2011; Miller *et al.* 2014; Sanderson *et al.* 2016). Calcineurin interacts with a segment in the proline-rich domain (aa 198–244; Yu *et al.* 2008), which encompasses the B-domain (S202–T231; Figs 1*A* and 8). If B-domain phosphorylation enhances tau-calcineurin binding affinity, then it is possible that the mislocalization of tau to dendritic spines would result in a greater concentration of calcineurin in the spines. This enhancement could lead to an increase in the internalization of GluA1 subunits of AMPA receptors dephosphorylated by calcineurin (Dell'Acqua *et al.* 2006; He *et al.* 2011; Sanderson *et al.* 2016). Supporting this idea, we previously showed that the calcineurin inhibitor FK-506 (tacrolimus) prevents tau-induced loss of functional

AMPA receptors in dendritic spines by blocking the dephosphorylation of GluA1 (Miller *et al.* 2014).

There are 85 putative phosphorylation residues in tau which vary in their extent of phosphorylation (Mair *et al.* 2016; Silva *et al.* 2016). Studies have used a mass-spectrometry-based assay to measure the stoichiometry of phosphorylated residues in soluble wild-type tau expressed in *Spodoptera frugiperda* (Sf9) cells and human neuronal induced pluripotent stem cells. The most frequently phosphorylated SP/TP residues were found to be S199, S202, T205, T212, T217, T231, S235, S396 and S404 (Mair *et al.* 2016; Silva *et al.* 2016). Specifically, ~85% of the wild-type tryptic fragments containing S396 and S404 were modified (reported as ~15% unmodified), indicating that one or both residues are phosphorylated in ~85% of wild-type tau molecules expressed and therefore should be mislocalized. It is puzzling why most wild-type tau proteins are not mislocalized in previous studies (Hoover *et al.* 2010; Ittner *et al.* 2010; Zhao *et al.* 2016). The stoichiometry of phosphorylation in primary neurons and the brain may differ from that in the insect and induced pluripotent stem cell culture paradigms. Support for this possibility includes the late appearance of staining of phosphorylated S396 and S404 with PHF-1 in humans with AD (Augustinack *et al.* 2002) and in a mouse model of frontotemporal dementia (Mair *et al.* 2016). Alternatively, there may be one or more ‘bottlenecks’ or rate-limiting steps controlled by other post-translational modifications of tau such as cleavage by caspase-2 (Zhao *et al.* 2016), acetylation by the major tau acetyltransferases CBP and p300 (Min *et al.* 2010; Tracy *et al.* 2016), and phosphorylation at non-SP/TP residues. One possible ‘bottleneck’ mechanism may be tau cleavage at Asp314 by caspase-2, which was previously shown to be necessary for the mislocalization of mutant P301L eGFP–tau (Zhao *et al.* 2016).

In summary, our findings define a common pathway in which the phosphorylation of residues in the C-terminal and proline-rich regions of tau regulates different steps leading to postsynaptic dysfunction. Several different post-translational modifications of tau must converge to cause synaptic deficits; these collectively form a cascade that plays a key role in the pathogenesis of Alzheimer’s disease and other tauopathies. We found that postsynaptic dysfunction does not result from the mislocalization of tau to dendritic spines *per se*, but dysfunction requires the additional phosphorylation of tau in another domain, which may reconcile some current conflicting results. For example, AAV-expressed Δtau314, a truncated species of tau that forms when caspase-2 cleaves tau at Asp314, mislocalizes to dendritic spines but does not impair cognition (Zhao *et al.* 2016). Our findings suggest that preventing either the mislocalization of tau or the reduction of AMPA receptors in dendritic spines—by targeting the specific phosphorylation sites characterized here—may result in promising therapies for Alzheimer’s disease and other tauopathies.

Acknowledgements

We would like to thank Drs Ben Smith and Xiaohui Zhao for their technical expertise and thoughtful discussions, and Beth Steuer for editing and formatting the manuscript. We also thank Chris Hlynialuk for providing technical assistance.

Funding

NIH Grant Numbers R21-NS084007–01 (D.L.); R21-NS096437–01 (D.L.); R01-NS79374 (K.H.A.); R01-AG60766 (K.H.A.); Michael J. Fox Foundation Grant (D.L.); UMN-Mayo Partnership Grant (D.L.); Minnesota Higher Education Grant (D.L.); Predoctoral Training Grant P32-GM008471 (E.M.).

Biography

Peter J. Teravskis received his BS in neuroscience and physiology (2012) from the University of Minnesota. He is currently enrolled in a joint degree (MD/JD) programme at the University of Minnesota Medical School and Law School. He is a medical student intern in Professor Liao's lab. Under the guidance of Professors Liao and Ashe, he researches neuronal synaptic pathology in translational models of dementia, Parkinson's disease and chronic traumatic encephalopathy. He is currently examining the mechanistic importance of caspase-2 cleavage of tau in the pathogenesis of frontotemporal dementia in a novel mouse model.

References

Augustinack JC, Schneider A, Mandelkow EM & Hyman BT (2002). Specific tau phosphorylation residues correlate with severity of neuronal cytopathology in Alzheimer's disease. Acta Neuropathol 103, 26–35. [PubMed: 11837744]

Avila J, Lucas JJ, Perez M & Hernandez F (2004). Role of tau protein in both physiological and pathological conditions. Physiol Rev 84, 361–384. [PubMed: 15044677]

Bhat RV, Budd Haeberlein SL & Avila J (2004). Glycogen synthase kinase 3: a drug target for CNS therapies. J Neurochem 89, 1313–1317. [PubMed: 15189333]

Braak H, Thal DR, Ghebremedhin E, Del Tredici K (2011).Stages of the pathologic process in Alzheimer disease: age categories from 1 to 100 years. J Neuropathol Exp Neurol 70, 960–969. [PubMed: 22002422]

Dell'Acqua ML, Smith KE, Gorski JA, Horne EA, Gibson ES & Gomez LL (2006). Regulation of neuronal PKA signaling through AKAP targeting dynamics. Eur J Cell Biol 85, 627–633. [PubMed: 16504338]

Ghetti B, Oblak AL, Boeve BF, Johnson KA, Dickerson BC & Goedert M (2015). Invited review: Frontotemporal dementia caused by microtubule-associated protein tau gene (MAPT) mutations: a chameleon for neuropathology and neuroimaging. Neuropathol Appl Neurobiol 41, 24–46. [PubMed: 25556536]

Goedert M, Jakes R & Vanmechelen E (1995). Monoclonal antibody AT8 recognises tau protein phosphorylated at both serine 202 and threonine 205. Neurosci Lett 189,167–169. [PubMed: 7624036]

Grueninger F, Bohrmann B, Christensen K, Graf M, Roth D & Czech C (2011). Novel screening cascade identifies MKK4 as key kinase regulating tau phosphorylation at Ser422. Mol Cell Biochem 357, 199–207. [PubMed: 21638028]

He K, Lee A, Song L, Kanold PO & Lee HK (2011). AMPA receptor subunit GluR1 (GluA1) serine-845 site is involved in synaptic depression but not in spine shrinkage associated with chemical long-term depression. J Neurophysiol 105, 1897–1907. [PubMed: 21307330]

Hoover BR, Reed MN, Su J, Penrod RD, Kotilinek LA, Grant MK, Pitstick R, Carlson GA, Lanier LM, Yuan LL, Ashe KH & Liao D (2010). Tau mislocalization to dendritic spines mediates synaptic dysfunction independently of neurodegeneration. Neuron 68, 1067–1081. [PubMed: 21172610]

Hutton M, Lendon CL, Rizzu P, Baker M, Froelich S, Houlden H, Pickering-Brown S, Chakraverty S, Isaacs A, Grover A, Hackett J, Adamson J, Lincoln S, Dickson D, Davies P, Petersen RC, Stevens M, de Graaff E, Wauters E, van Baren J, Hillebrand M, Joosse M, Kwon JM, Nowotny P, Che LK, Norton J, Morris JC, Reed LA, Trojanowski J, Basun H, Lannfelt L, Neystat M, Fahn S, Dark F, Tannenberg T, Dodd PR, Hayward N, Kwok JB, Schofield PR, Andreadis A, Snowden J, Craufurd D, Neary D, Owen F, Oostra BA, Hardy J, Goate A, van Swieten J, Mann D, Lynch T & Heutink P (1998). Association of missense and 5′-splice-site mutations in tau with the inherited dementia FTDP-17. Nature 393, 702–705. [PubMed: 9641683]

Illenberger S, Zheng-Fischhöfer Q, Preuss U, Stamer K, Baumann K, Trinczek B, Biernat J, Godemann R, Mandelkow EM & Mandelkow E (1998). The endogenous and cell cycle-dependent phosphorylation of tau protein in living cells: implications for Alzheimer's disease. Mol Biol Cell 9, 1495–1512. [PubMed: 9614189]

Ittner LM, Ke YD, Delerue F, Bi M, Gladbach A, van Eersel J, Wölfing H, Chieng BC, Christie MJ, Napier IA, Eckert A, Staufenbiel M, Hardeman E, Götz J (2010). Dendritic function of tau mediates amyloid-β toxicity in Alzheimer's disease mouse models. Cell 142, 387–397. [PubMed: 20655099]

Kam AY, Liao D, Loh HH & Law PY (2010). Morphine induces AMPA receptor internalization in primary hippocampal neurons via calcineurin-dependent dephosphorylation of GluR1 subunits. J Neurosci 30, 15304–15316. [PubMed: 21068335]

Kim E, Sakata K, Liao FF (2017). Bidirectional interplay of HSF1 degradation and UPR activation promotes tau hyperphosphorylation. PLoS Genet 13, e1006849. [PubMed: 28678786]

Kimura T, Ishiguro K & Hisanaga S (2014). Physiological and pathological phosphorylation of tau by Cdk5. Front Mol Neurosci 7, 65. [PubMed: 25076872]

Kowall NW & Kosik KS (1987). Axonal disruption and aberrant localization of tau protein characterize the neuropil pathology of Alzheimer's disease. Ann Neurol 22, 639–643. [PubMed: 3122646]

Lai E, Teodoro T & Volchuk A (2007). Endoplasmic reticulum stress: signaling the unfolded protein response. Physiology (Bethesda) 22, 193–201. [PubMed: 17557940]

Lasagna-Reeves CA, Castillo-Carranza DL, Sengupta U, Clos AL, Jackson GR & Kayed R (2011). Tau oligomers impair memory and induce synaptic and mitochondrial dysfunction in wild-type mice. Mol Neurodegener 6, 39. [PubMed: 21645391]

Liao D, Lin H, Law PY & Loh HH (2005). Mu-opioid receptors modulate the stability of dendritic spines. Proc Natl Acad Sci U S A 102, 1725–1730. [PubMed: 15659552]

Lin H, Huganir R & Liao D (2004). Temporal dynamics of NMDA receptor-induced changes in spine morphology and AMPA receptor recruitment to spines. Biochem Biophys Res Commun 316, 501–511. [PubMed: 15020245]

Liu ZC, Chu J, Lin L, Song J, Ning LN, Luo HB, Yang SS, Shi Y, Wang Q, Qu N, Zhang Q, Wang JZ & Tian Q (2016). SIL1 rescued Bip elevation-related tau hyperphosphorylation in ER stress. Mol Neurobiol 35, 983–994.

Maday S, Twelvetrees AE, Moughamian AJ & Holzbaur EL (2014). Axonal transport: cargo-specific mechanisms of motility and regulation. Neuron 84, 292–309. [PubMed: 25374356]

Mair W, Muntel J, Tepper K, Tang S, Biernat J, Seeley WW, Kosik KS, Mandelkow E, Steen H & Steen JA (2016). FLEXITau: quantifying post-translational modifications of tau protein *in vitro* and in human disease. Anal Chem 88, 3704–3714. [PubMed: 26877193]

McInnes J, Wierda K, Snellinx A, Bounti L, Wang YC, Stancu IC, Apóstolo N, Gevaert K, Dewachter I, Spires-Jones TL, De Strooper B, De Wit J, Zhou L & Verstreken P (2018). Synaptogyrin-3 mediates presynaptic dysfunction induced by tau. Neuron 97, 823–835. [PubMed: 29398363]

McKee AC, Cantu RC, Nowinski CJ, Hedley-Whyte ET, Gavett BE, Budson AE, Santini VE, Lee HS, Kubilus CA & Stern RA (2009). Chronic traumatic encephalopathy in athletes: progressive tauopathy after repetitive head injury. J Neuropathol Exp Neurol 68,709–735. [PubMed: 19535999]

Miller EC, Teravskis PJ, Dummer BW, Zhao X, Huganir RL & Liao D (2014). Tau phosphorylation and tau mislocalization mediate soluble Aβ oligomer-induced AMPA glutamate receptor signaling dysfunctions. Eur J Neurosci 39, 1214–1224. [PubMed: 24713000]

Min SW, Cho SH, Zhou Y, Schroeder S, Haroutunian V, Seeley WW, Huang EJ, Shen Y, Masliah E, Mukherjee C, Meyers D, Cole PA, Ott M & Gan L (2010). Acetylation of tau inhibits its degradation and contributes to tauopathy. Neuron 67, 953–966. [PubMed: 20869593]

Montenigro PH, Bernick C & Cantu RC (2015). Clinical features of repetitive traumatic brain injury and chronic traumatic encephalopathy. Brain Pathol 25,304–17. [PubMed: 25904046]

Patrick GN, Zukerberg L, Nikolic M, de la Monte S, Dikkes P & Tsai LH (1999). Conversion of p35 to p25 deregulates Cdk5 activity and promotes neurodegeneration. Nature 402, 615–622. [PubMed: 10604467]

Ramsden M, Kotilinek L, Forster C, Paulson J, McGowan E, SantaCruz K, Guimaraes A, Yue M, Lewis J, Carlson G, Hutton M & Ashe KH (2005). Age-dependent neurofibrillary tangle formation, neuron loss, and memory impairment in a mouse model of human tauopathy (P301L). J Neurosci 25, 10637–10647. [PubMed: 16291936]

Sanderson JL, Gorski JA, Dell'Acqua ML (2016). NMDA receptor-dependent LTD requires transient synaptic incorporation of Ca^{2+}-permeable AMPARs mediated by AKAP150-anchored PKA and calcineurin. Neuron 89, 1000–1015. [PubMed: 26938443]

Santacruz K, Lewis J, Spires T, Paulson J, Kotilinek L, Ingelsson M, Guimaraes A, DeTure M, Ramsden M, McGowan E, Forster C, Yue M, Orne J, Janus C, Mariash A, Kuskowski M, Hyman B, Hutton M & Ashe KH (2005). Tau suppression in a neurodegenerative mouse model improves memory function. Science 309, 476–481. [PubMed: 16020737]

Sealey MA, Vourkou E, Cowan CM, Bossing T, Quraishe S, Grammenoudi S, Skoulakis EMC & Mudher A (2017). Distinct phenotypes of three-repeat and four-repeat human tau in a transgenic model of tauopathy. Neurobiol Dis 105, 74–83. [PubMed: 28502805]

Sherman MA, LaCroix M, Amar F, Larson ME, Forster C, Aguzzi A, Bennett DA, Ramsden M & Lesne SE (2016). Soluble conformers of Aβ and tau alter selective proteins governing axonal transport. J Neurosci 36, 9647–9658. [PubMed: 27629715]

Shukla V, Skuntz S & Pant HC (2012). Deregulated Cdk5 activity is involved in inducing Alzheimer's disease. Arch Med Res 43, 655–662. [PubMed: 23142263]

Silva MC, Cheng C, Mair W, Almeida S, Fong H, Biswas MHU, Zhang Z, Huang Y, Temple S, Coppola G, Geschwind DH, Karydas A, Miller BL, Kosik KS, Gao FB, Steen JA & Haggarty SJ (2016). Human iPSC-derived neuronal model of tau-A152T frontotemporal dementia reveals tau-mediated mechanisms of neuronal vulnerability. Stem Cell Reports 7, 325–340. [PubMed: 27594585]

Su KH, Cao J, Tang Z, Dai S, He Y, Sampson SB, Benjamin IJ & Dai C (2016). HSF1 critically attunes proteotoxic stress sensing by mTORC1 to combat stress and promote growth. Nat Cell Biol 18, 527–539. [PubMed: 27043084]

Sydow A, Van der Jeugd A, Zheng F, Ahmed T, Balschun D, Petrova O, Drexler D, Zhou L, Rune G, Mandelkow E, D'Hooge R, Alzheimer C & Mandelkow EM (2011). Tau-induced defects in synaptic plasticity, learning, and memory are reversible in transgenic mice after switching off the toxic tau mutant. J Neurosci 31, 2511–2525. [PubMed: 21325519]

Tenreiro S, Eckermann K & Outeiro TF (2014). Protein phosphorylation in neurodegeneration: friend or foe? Front Mol Neurosci 7, 42. [PubMed: 24860424]

Tracy TE & Gan L (2018). Tau-mediated synaptic and neuronal dysfunction in neurodegenerative disease. Curr Opin Neurobiol 51, 134–138. [PubMed: 29753269]

Tracy TE, Sohn PD, Minami SS, Wang C, Min SW, Li Y, Zhou Y, Le D, Lo I, Ponnusamy R, Cong X, Schilling B, Ellerby LM, Huganir RL & Gan L (2016). Acetylated tau obstructs KIBRA-mediated signaling in synaptic plasticity and promotes tauopathy-related memory loss. Neuron 90, 245–260. [PubMed: 27041503]

Yu DY, Tong L, Song GJ, Lin WL, Zhang LQ, Bai W, Gong H, Yin YX & Wei Q (2008). Tau binds both subunits of calcineurin, and binding is impaired by calmodulin. Biochim Biophys Acta 1783, 2255–2261. [PubMed: 18639592]

Zempel H & Mandelkow E (2014). Lost after translation: missorting of Tau protein and consequences for Alzheimer disease. Trends Neurosci 37, 721–732. [PubMed: 25223701]

Zhao X, Kotilinek LA, Smith B, Hlynialuk C, Zahs K, Ramsden M, Cleary J & Ashe KH (2016). Caspase-2 cleavage of tau reversibly impairs memory. Nat Med 22, 1268–1276. [PubMed: 27723722]

Zhou L, McInnes J, Wierda K, Holt M, Herrmann AG, Jackson RJ, Wang YC, Swerts J, Beyens J, Miskiewicz K, Vilain S, Dewachter I, Moechars D, De Strooper B, Spires-Jones TL, De Wit J & Verstreken P (2017). Tau association with synaptic vesicles causes presynaptic dysfunction. Nat Commun 8, 15295. [PubMed: 28492240]

Key points

- Tau mislocalization to dendritic spines and associated postsynaptic deficits are mediated through different and non-overlapping phosphorylation sites.
- Tau mislocalization to dendritic spines depends upon the phosphorylation of either Ser396 or Ser404 in the C-terminus.
- Postsynaptic dysfunction instead depends upon the phosphorylation of at least one of five residues in the proline-rich region of tau.
- The blockade of both glycogen synthetase kinase 3β and cyclin-dependent kinase 5 is required to prevent P301L-induced tau mislocalization to dendritic spines, supporting redundant pathways that control tau mislocalization to spines.

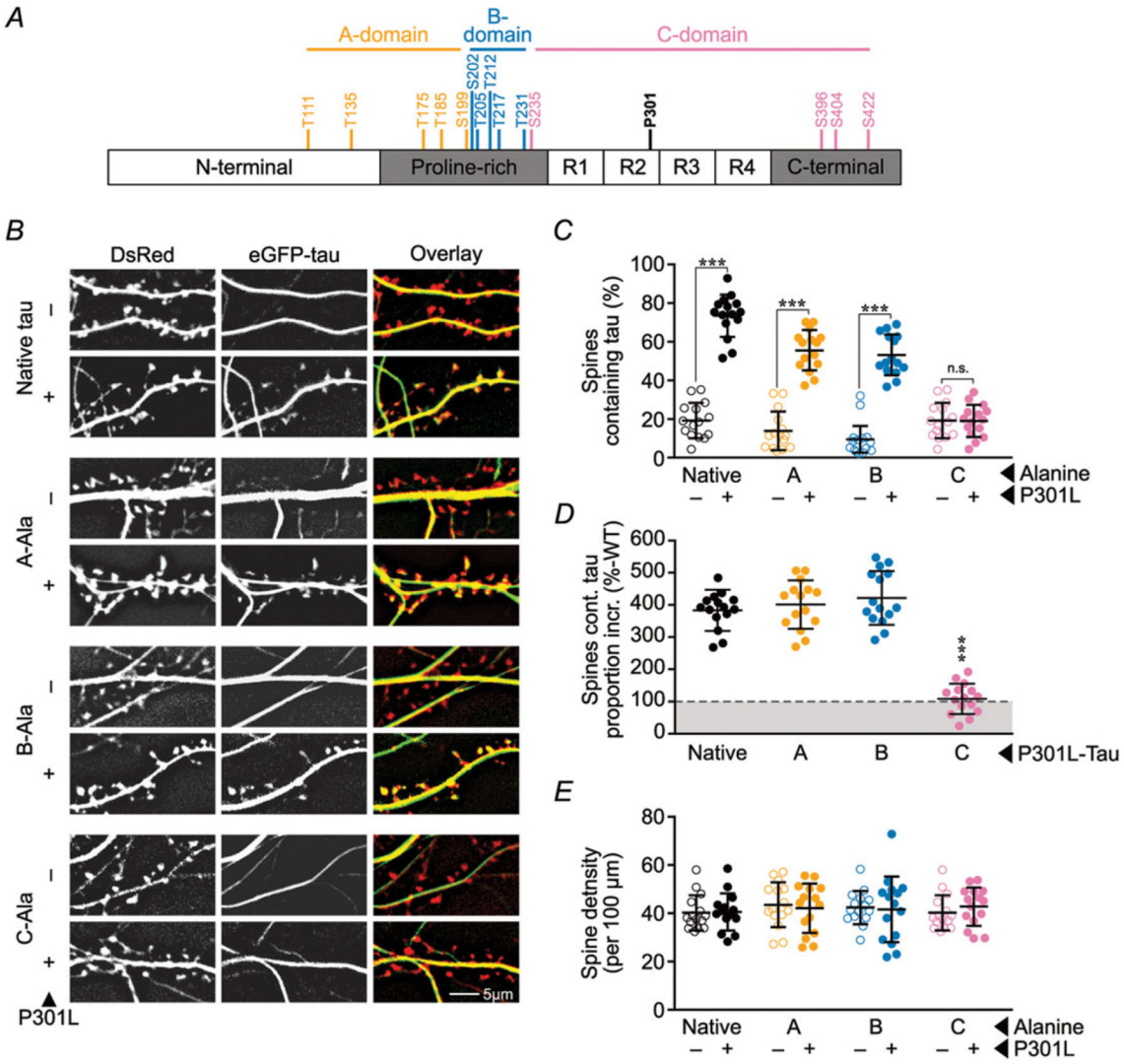

Figure 1. Blocking phosphorylation of C-domain residues reduces the mislocalization of P301L mutant tau to dendritic spines

A, map of A-, B- and C-domains of tau (coloured orange, blue and pink, respectively; Fig. 8 shows the rationale for this grouping). *B*, representative images of eGFP–tau constructs (green) and DsRed (red) expressed in rat primary hippocampal neuronal cultures. Tau expressing the P301L mutation mislocalizes to a majority of spines, except when C-residues are mutated to alanine to block phosphorylation. '–' refers to wild-type tau without a P301L mutation and 'native' refers to tau lacking mutations of the A-, B- or C- residues. '-Ala' indicates mutation to alanine. *C*, quantification of percentage of spines containing tau. *D*, spines containing P301L mutant eGFP–tau normalized to respective wild-type alanine variants to estimate the amount of tau missorting. *E*, quantification of total spine density. In *C* and *E*, data were analysed by two-way ANOVA shielded Bonferroni *post hoc* analysis. In *C*, $F_{(3, 112)} = 49.24$; Native, A, B: ***$P < 0.0001$, C: n.s. $P > 0.9999$. In *E*, $F_{(3, 112)} = 0.277$. In *D*, data were analysed by one-way ANOVA shielded Bonferroni *post hoc* analysis; $F_{(3, 56)} = 72.03$; ***$P < 0.0001$. For all, error bars represent mean ± SD; $n = 15$ neurons.

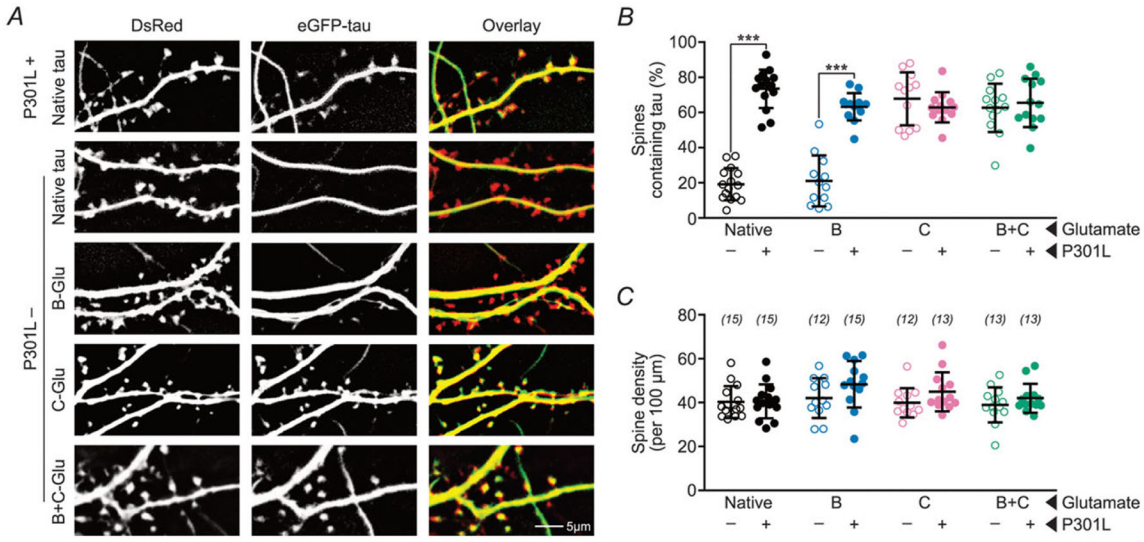

Figure 2. Pseudophosphorylation of C-domain residues enhances the mislocalization of wild-type tau to dendritic spines

A, representative photomicrographs of eGFP–tau constructs (green) and DsRed (red) expressed in rat primary hippocampal neuronal cultures. '-Glu' indicates glutamate substitutions of S/T residues to mimic phosphorylation in the respective domains. The mislocalization of tau with pseudophosphorylated C-residues (4th row) is comparable to that of P301L mutant tau (1st row). The addition of B-Glu mutations to tau with C-Glu mutations does not further increase the mislocalization of tau (5th row). *B*, quantification of percentage of spines containing tau. *C*, quantification of total spine density. Data were analysed by two-way ANOVA shielded Bonferroni *post hoc* analysis. In *B*, $F_{(3, 98)} = 40.45$; $^{***}P < 0.0001$. In *C*, $F_{(3, 98)} = 0.699$. *n* (number of neurons) is represented in parentheses. Error bars represent mean ± SD.

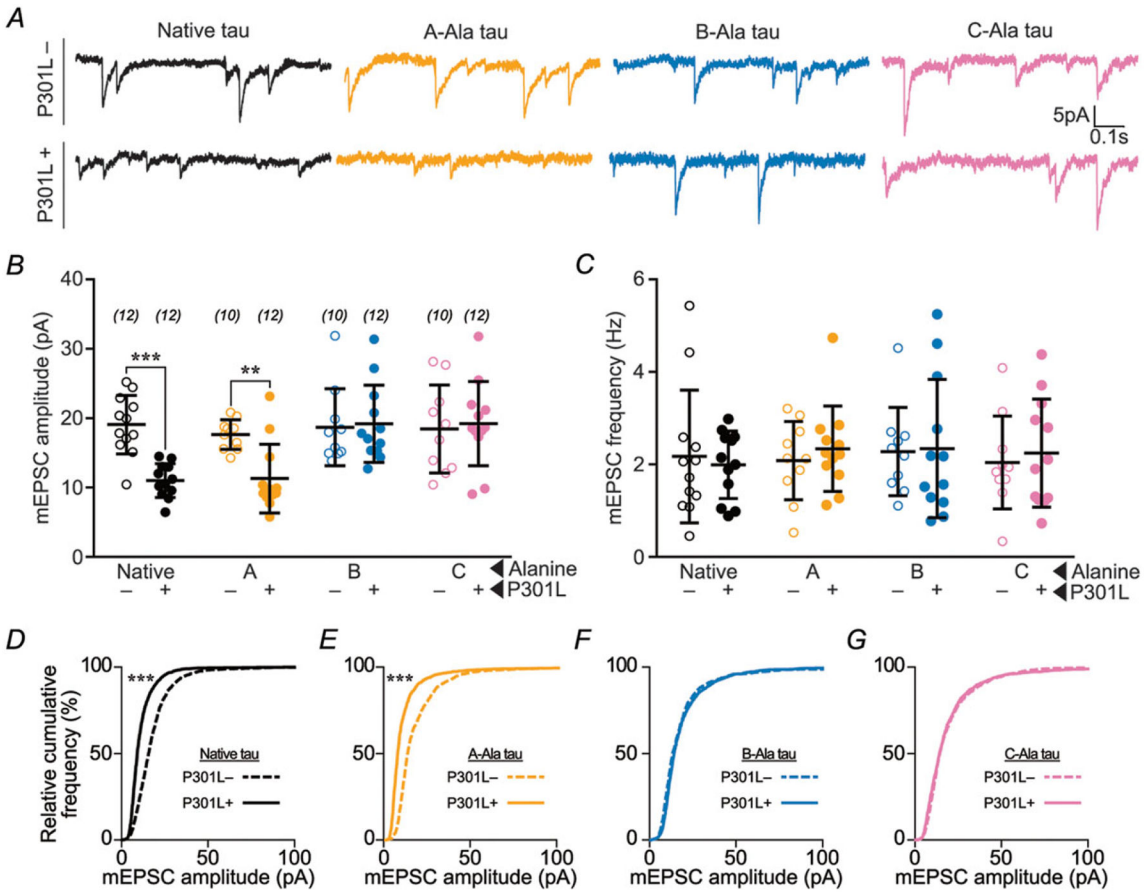

Figure 3. Blocking phosphorylation of B- or C-domain residues prevents P301L mutant tau-induced glutamatergic postsynaptic deficits

A, representative traces of rat hippocampal neurons transfected with eGFP–tau constructs. Neurons were bathed in ACSF containing TTX (1 μM), picrotoxin (100 μM), and APV (100 μM) to isolate AMPA receptor mEPSCs. P301L mutant tau-containing constructs led to a reduction in mEPSC amplitude, except when either the B-residues or the C-residues were mutated to alanine to prevent phosphorylation. *B*, quantification of mEPSC amplitudes. *C*, quantification of mEPSC frequencies. *D*–*G*, relative cumulative frequency of amplitudes of all mEPSC events in multiple groups. In *B* and *C*, data were analysed by two-way ANOVA shielded Bonferroni *post hoc* analysis. In *B*, $F_{(3, 79)} = 5.082$; native: ***$P = 0.0005$, A: *$P = 0.0179$. In *C*, $F_{(3, 79)} = 0.4394$. In *D*–*G*, data were analysed by the Kolmogorov–Smirnov GOF test; ***$P < 0.0001$. Error bars represent mean ± SD. *n* (number of neurons) is represented in parentheses.

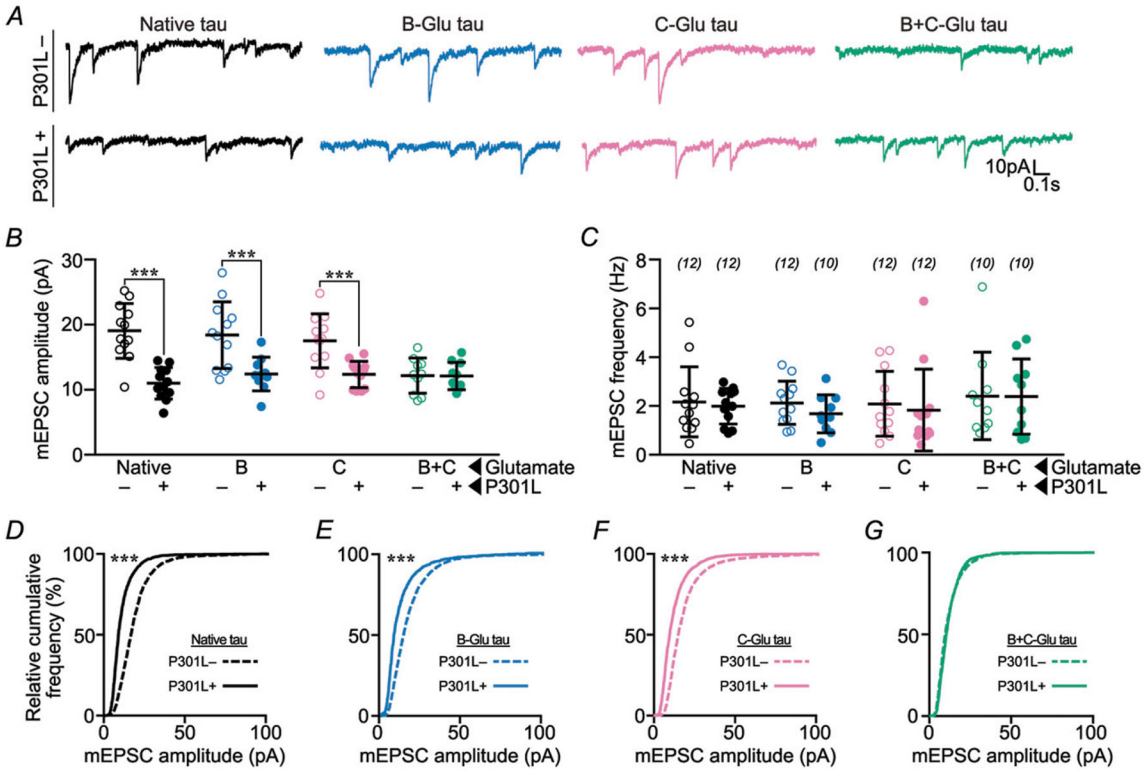

Figure 4. Pseudophosphorylation of B- and C-domain residues combined induces glutamatergic post-synaptic deficits

A, representative traces of rat hippocampal neurons transfected with eGFP–tau constructs. Neurons were bathed in ACSF as before to isolate AMPA receptor mEPSCs. All P301L mutant tau-containing constructs show reduced mEPSC amplitudes. Pseudophosphorylation in a single domain does not induce deficits; however, pseudo-phosphorylation of both B- and C-residues in combination reduced mEPSC amplitudes. *B*, quantification of mEPSC amplitudes. *C*, quantification of mEPSC frequencies. *D*–*G*, relative cumulative frequency of amplitudes of all mEPSC events in multiple groups. In *B* and *C*, data were analysed by two-way ANOVA shielded Bonferroni *post hoc* analysis. In *B*, $F_{(3, 76)} = 3.406$; Native: ***$P <$ 0.0001, B: ***$P = 0.0004$, C: **$P = 0.0015$. In *C*, $F_{(3, 76)} = 0.5672$. In *D*–*G*, data were analysed by the Kolmogorov–Smirnov GOF test; ***$P < 0.0001$. Error bars represent mean ± SD. *n* (number of neurons) is represented in parentheses.

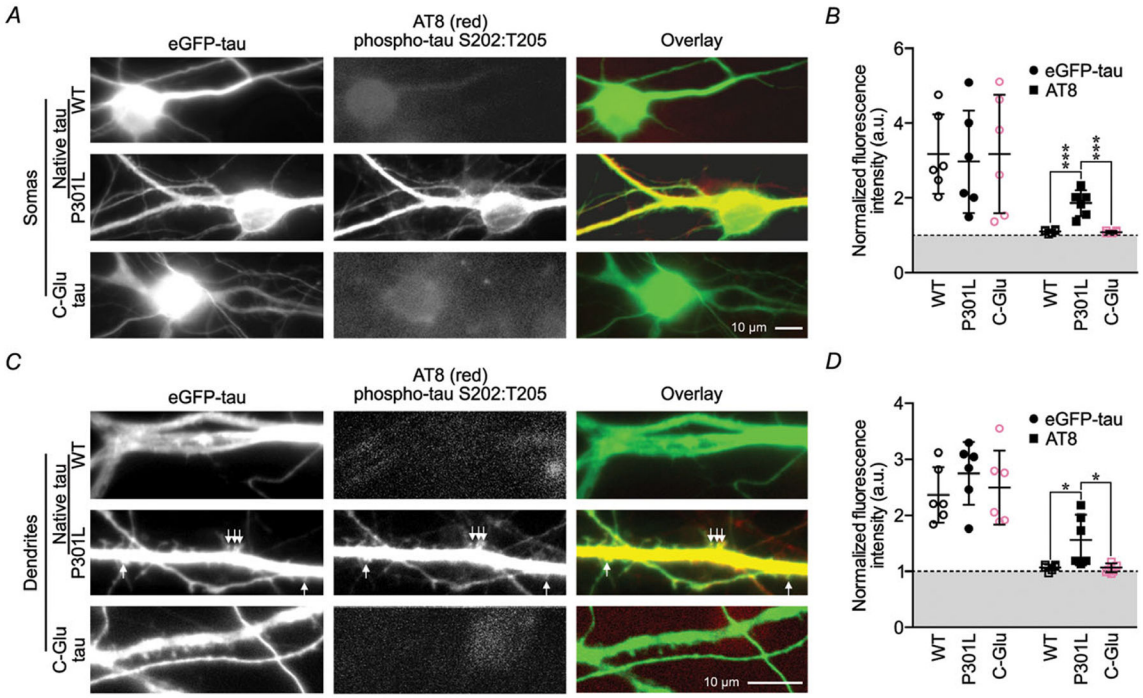

Figure 5. Pseudophosphorylation of C-domain residues is not sufficient to induce phosphorylation of the complete set of B-domain residues

A, representative photomicrographs of neuronal somas expressing native wild-type or P301L eGFP–tau, and neurons expressing variant C-Glu eGFP–tau stained for S202 and T205 phosphorylation with AT8 antibodies. *B*, quantification of somatic eGFP and AT8 luminance normalized to background fluorescence. *C*, representative photomicrographs of dendrites from neurons presented in *A*. *D*, quantification of dendritic eGFP and AT8 fluorescence luminance normalized to background fluorescence. All data were analysed by two-way ANOVA shielded Bonferroni *post hoc* analysis. For *B*, $F_{(1, 30)} = 29.57$; $P < 0.0001$. In *D*, $F_{(1, 30)} = 76.51$; wild-type and C-Glu $P = 0.017$. For all, $n = 6$ neurons; error bars represent mean ± SD.

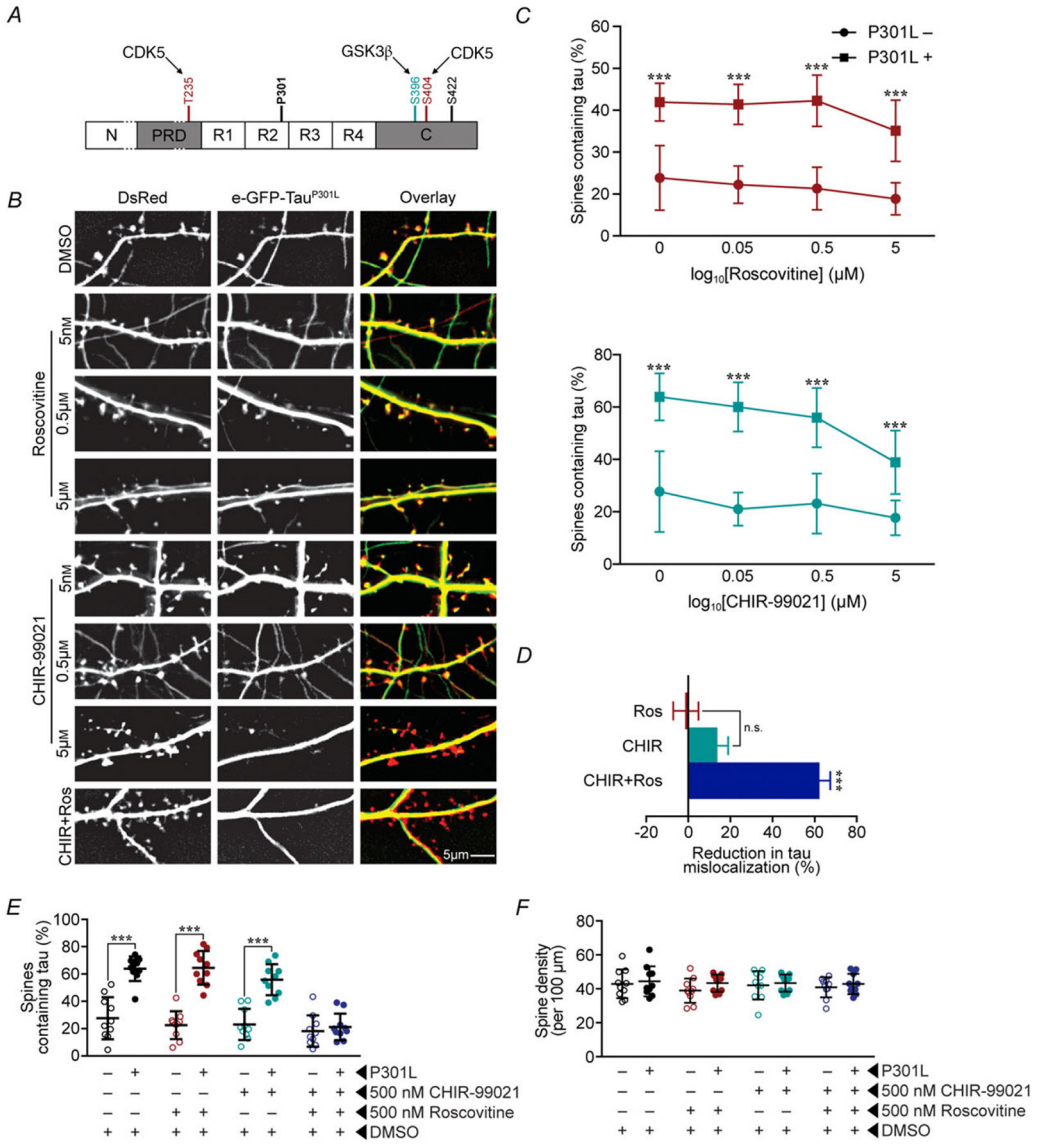

Figure 6. Blocking mislocalization of P301L mutant tau requires the inhibition of both GSK3*β* and CDK5

A, schematic representation of C-residues. Maroon colour (S235 and S404) indicates residues phosphorylated by CDK5; teal colour (S396) indicates residues phosphorylated by GSK3*β*. *B*, representative images of neurons treated by control vehicle DMSO, CDK5 inhibitor roscovitine (Ros) alone, GSK3*β* inhibitor CHIR99021 (CHIR) alone and CHIR + Ros. *C*, dose–response curves of Ros and CHIR on percentage of spines containing tau in neurons that express eGFP–tau constructs (green) and DsRed (red). These results indicate that inhibition of either GSK3*β* or CDK5 alone is insufficient to block P301L mutation-induced tau mislocalization to dendritic spines. *D*, percentage of spines containing tau in neurons that had been treated with 500 nM roscovitine (CDK inhibitor) and/or CHIR99021 (GSK3*β* inhibitor). *E*, percentage reduction in mislocalization from untreated P301L-tau by each drug treatment regime. Results in *D* and *E* demonstrate that blocking both GSK3*β* and CDK5 kinases is required to block tau mislocalization. *F*, quantification of total spine

density in neurons with different treatment paradigms, showing no overt loss of dendritic spines. Data were analysed by one-way ANOVA shielded Bonferroni *post hoc* analysis. ***$P < 0.0001$; $n = 10$ neurons; error bars represent mean ± SD.

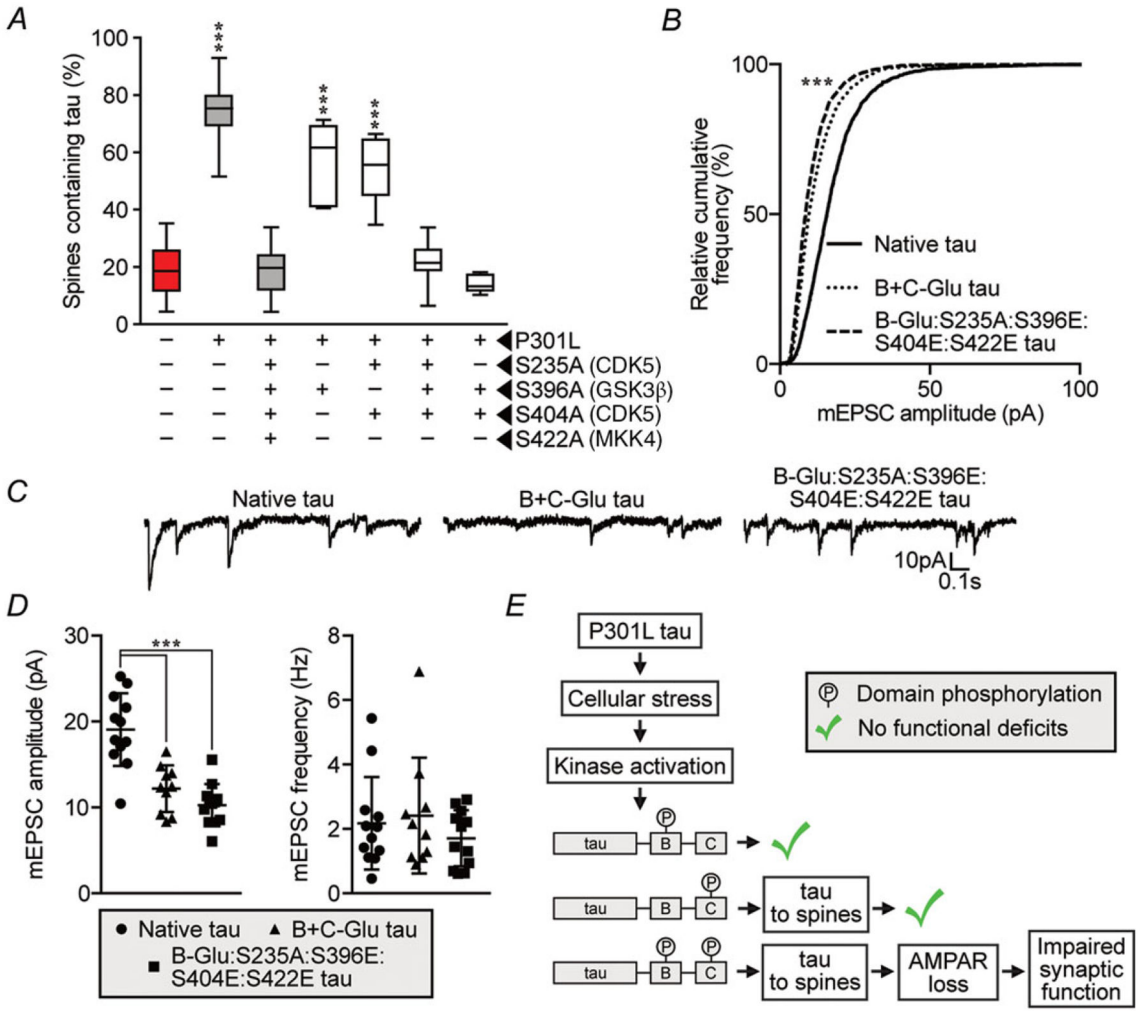

Figure 7. Blocking phosphorylation of S396 and S404 together prevents P301L mutant tau-induced mislocalization, but blocking phosphorylation of S235 in the proline-rich region has no effect on synaptic dysfunction

A, systematic mutagenesis of C-residues shows that blocking phosphorylation of S396 and S404 together prevents P301L mutant tau-induced mislocalization, but blocking either S396 or S404 alone does not prevent mislocalization. Data were analysed by one-way ANOVA shielded Bonferroni *post hoc* analysis. $F_{(6, 65)} = 74.32$; *** $P < 0.001$; $n = 6–15$ neurons; error bars represent mean ± 95% CI. *B*, relative cumulative frequency of amplitudes of all mEPSC events in each group. Data were analysed by Kolmogorov–Smirnov GOF test. $D = 0.318$; *** $P = 0.0004$. *C*, representative traces. *D*, event amplitudes and frequencies for mEPSCs described in *B* and *C*. Data were analysed by one-way ANOVA shielded Bonferroni *post hoc* analysis. $F_{(2, 31)} = 2.332$; *** $P < 0.0001$; $n = 10–12$ neurons; error bars represent mean ± SD. *E*, diagram illustrating a hypothetical model that integrates the interaction between phosphorylation by protein kinases GSK3*β* and CDK5. Kinases activated by P301L mutant tau must phosphorylate residues in the B- *and* C-domains for mislocalization and synaptic deficits to occur.

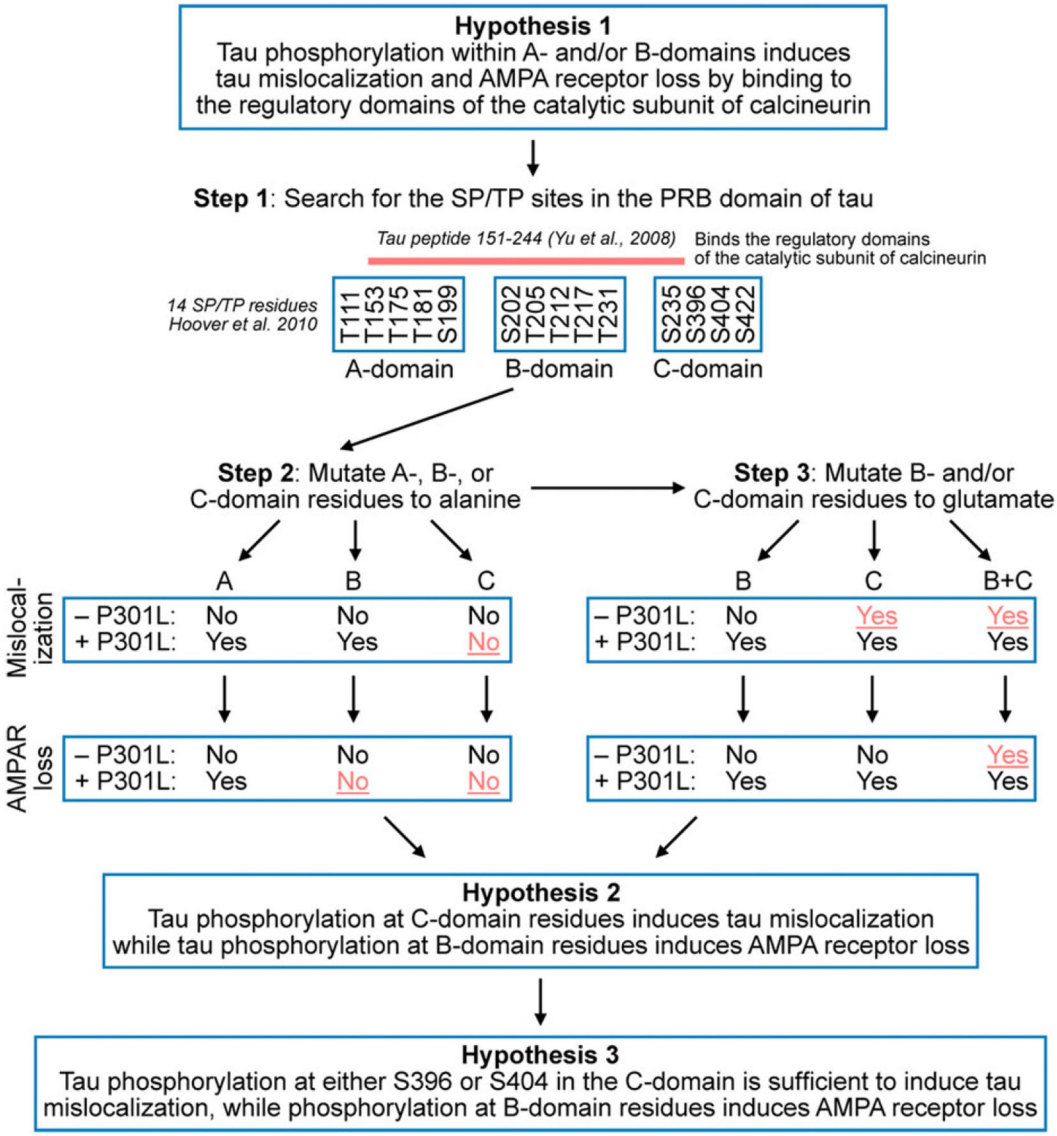

Figure 8. Evolution of hypotheses pertaining to the role of phosphorylation on postsynaptic dysfunction

We partitioned tau based on our initial hypothesis (Hypothesis 1) that SP/TP residues in the A-domain and/or B-domain activate calcineurin leading to the internalization of AMPA receptors causing postsynaptic dysfunction (Step 1). The scientific rationale for this hypothesis was based on our own studies (Hoover *et al.* 2010; Miller *et al.* 2014) and a published observation describing the interaction of a segment (aa 198–244) of the proline rich region of tau (aa 151–244) with the regulatory domains of the catalytic subunit of calcineurin (Yu *et al.* 2008). To test this hypothesis, we mutated SP/TP residues in the A-, B- or C-domains of wild-type or P301L mutant tau to alanine to block phosphorylation (Step 2). We found that the phosphorylation state of A-residues was neither necessary (Fig. 3) nor sufficient to cause synaptic deficits (Fig. 9). Next, we characterized the B- and C-domains further by producing tau variants with phosphomimetic substitutions in these domains (Step

3). Based on results shown in Figs 1–4, we revised Hypothesis 1 and generated Hypothesis 2. The findings in Figs 6–7 led us to Hypothesis 3, a refinement of Hypothesis 2.

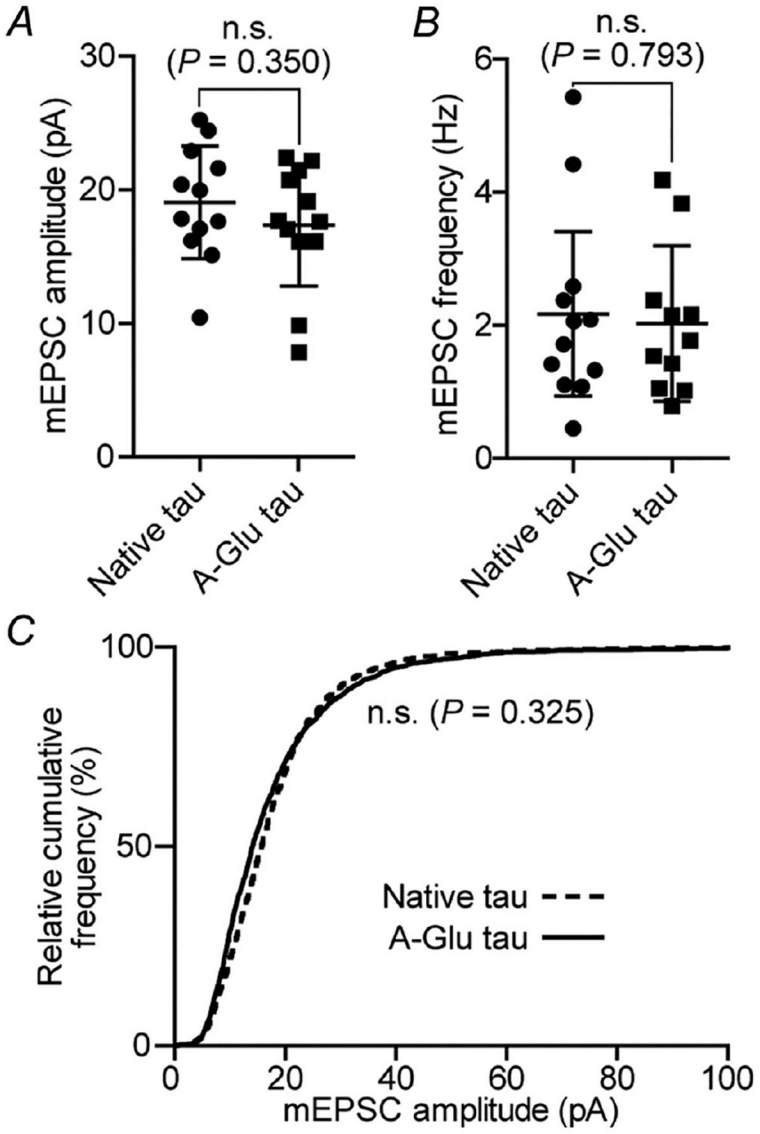

Figure 9. Analyses of mEPSCs recorded in neurons expressing A-Glu tau

A, comparison of mEPSC amplitudes in neurons expressing native tau and the A-Glu variant (neither contains the P301L mutation). *B*, quantification of mEPSC frequencies. *C*, relative cumulative frequency of amplitudes of all mEPSC events in both groups. These results indicate that phosphorylation of A-domain alone is not sufficient to cause synaptic deficits. The results here and the results in Fig. 3 suggest that the phosphorylation of A-domain residues plays a minimal role in tau-induced synaptic deficits over the time period observed (11–14 days after transfection). However, whether the A-domain is involved in spine loss or cell death at later stages remains to be determined. In *A* and *B*, data were analysed with Student's *t* test; $n = 12$ neurons; error bars are mean ± SD. In *C*, data were analysed by the Kolmogorov–Smirnov GOF test.